

N O T I C E

THIS DOCUMENT HAS BEEN REPRODUCED FROM
MICROFICHE. ALTHOUGH IT IS RECOGNIZED THAT
CERTAIN PORTIONS ARE ILLEGIBLE, IT IS BEING RELEASED
IN THE INTEREST OF MAKING AVAILABLE AS MUCH
INFORMATION AS POSSIBLE

EXTENSION OF OBLIQUE INCIDENCE METHOD
TO PHOTO-ORTHOTROPIC-ELASTICITY

Paper describes the separation of principal stresses in transversely isotropic birefringent composite models by the oblique incidence method

R. Prabhakaran

Associate Professor

Department of Mechanical Engineering & Mechanics

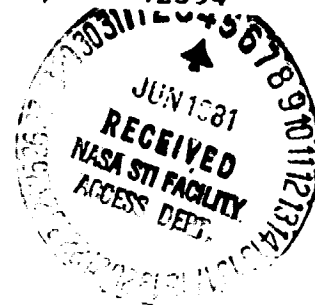
Old Dominion University

Norfolk, Virginia 23508

(NASA-CR-164334) EXTENSION OF OBLIQUE
INCIDENCE METHOD TO
PHOTO-ORTHOTROPIC-ELASTICITY (Old Dominion
Univ., Norfolk, Va.) 22 p HC A02/MF A01

N81-23492

Unclas
42394
CSCL 20K G3/39



ABSTRACT

With the interpretation of isochromatic and isoclinic fringes in transparent, birefringent, orthotropic composites established, efforts have been in progress to determine the individual values of the principal stresses or strains. Several methods have recently been proposed. Some of them utilize the photoelastic results only partially and rely on numerical procedures. Others have attempted to obtain the required information based entirely on experimental data. In this paper, the classical oblique incidence technique is applied to transversely isotropic birefringent composites. The proposed extension is verified by applying it to the problem of an orthotropic half-plane subjected to an edge-load.

NOMENCLATURE

E	Young's modulus
f	stress-fringe value
h	thickness
k	derived elastic constant
N	isochromatic fringe order
P	load
u	derived elastic constant
x,y	cartesian coordinates
σ	normal stress
τ	shear stress
θ	angle of oblique incidence
θ'	optical isoclinic angle
ν	Poisson's ratio

Subscripts

L	direction along the reinforcement
n	normal incidence
T	direction perpendicular to the reinforcement
θ	oblique incidence, corresponding to angle θ
x,y	along the coordinate axes

INTRODUCTION

Continuous fiber reinforced composites are heterogenous and exhibit several modes of failure such as matrix crazing, delamination, fiber failure and interfacial bond failure. Therefore stress analysis and failure analysis based on micromechanics considerations appear more realistic. However, such analyses are not only complex, but also difficult to apply in design. Macromechanics analyses, such as failure theories and fracture mechanics, treat the composite as a continuum with anisotropic properties. The results from such simplified analyses are easy to apply in design and have been shown to agree with experimental results, at least in some cases. A macromechanics treatment of composites requires the individual values of the stress components.

Photoelasticity is well established as a useful whole-field method of obtaining principal or shear stresses in isotropic models or structures. Considerable progress has been achieved in the application of transmission photoelastic techniques to composite orthotropic model materials in recent years. The developments in the subject have been reviewed by Prabhakaran^(1,2). The interpretation of the photoelastic response is not straight-forward, in terms of stresses or strains. The isochromatic fringe order is a complex function of the principal stresses (or strains), their orientation, etc. For a balanced ($f_L = f_T$) material, the fringe order is proportional to the difference in principal stresses (or strains); for an unbalanced laminate, when the principal stress (or strain) directions coincide with the material symmetry axes, the fringe order is a linear function of the principal stresses (or strains). The isoclinic fringes give the directions of the principal birefringence components according to a Mohr circle of birefringence; the principal strain directions are a better approximation to the isoclinic parameter than are the principal stress

directions. It is, therefore, clear that for the transmission photoelastic analysis of an orthotropic model to yield useful information, methods must be developed to determine the individual values of principal stresses (or strains).

Several methods have already been proposed for this purpose. The application of the shear difference method to orthotropic models in conjunction with an approximate strain-optic law was suggested by Hayashi⁽³⁾ and was later developed and utilised by Netrebko⁽⁴⁾ and Netrebko and Zlenko⁽⁵⁾. Sampson⁽⁶⁾ proposed that the components of birefringence according to the Mohr circle of birefringence, along with the differential equations of equilibrium, be used in a shear difference method for separating the principal stresses. Knight and Pih⁽⁷⁾ developed the method and applied it to the solution of an orthotropic tensile strip with a circular hole. Chandrasekhara and Abraham^(8,9) combined the photoelastic results on the boundary with the numerical solution of the compatibility equation, for the special case when the material- and model- symmetry axes were coincident. Rowlands and co-workers⁽¹⁰⁾ obtained the isopachic and isochromatic fringes by transmission holography for an orthotropic plate with a central crack and concluded that in general this method of stress separation was difficult. Prabhakaran⁽¹¹⁾ has proposed that the transmission and reflection photoelastic methods be combined to obtain the individual values of the principal stress (or strain). Prabhakaran⁽¹²⁾ has also extended the method of drilling small holes to orthotropic birefringent models. In this paper, the oblique incidence method is applied to unidirectionally reinforced birefringent composite models.

OBLIQUE INCIDENCE METHOD FOR TRANSVERSELY ISOTROPIC
MODELS

In the case of isotropic photoelastic models or coatings, the model (or the specimen with the photoelastic coating) is usually rotated about one of the principal stress (or strain) directions. The isoclinic parameter in such situations identifies the principal directions at a point. In the case of orthotropic photoelastic models, the principal stress direction is not given by the optical isoclinic and therefore rotation of the model about a principal stress direction is not possible. It is, however, possible to rotate the model about a principal strain direction if it is assumed that the isoclinic parameter approximately indicates the principal strain direction. But the resulting equations are very complex.

Simplification is achieved in the case of a transversely isotropic birefringent model if the state of stress at any point is expressed in terms of the three in-plane stress components referred to the material symmetry axes σ_L , σ_T and τ_{LT} . The normal incidence isochromatic fringe order can be expressed in terms of these stress components as

$$N_n = h \left\{ \left(\frac{\sigma_L}{f_L} - \frac{\sigma_T}{f_T} \right)^2 + \left(\frac{2\tau_{LT}}{f_{LT}} \right)^2 \right\}^{1/2} \quad (1)$$

where f_L , f_T and f_{LT} are the principal stress-fringe values and h is the model thickness. According to the Mohr circle of birefringence, the optical isoclinic parameter, θ' , is related to the stress components by

$$\tan 2\theta' = \frac{2\tau_{LT}/f_{LT}}{\frac{\sigma_L}{f_L} - \frac{\sigma_T}{f_T}} \quad (2)$$

Let the model be rotated about the L-axis, which is the fiber direction, by an angle θ as shown in Fig. 1. The oblique incidence fringe order is given by

$$N_{\theta} = \frac{h}{\cos\theta} \left\{ \left(\frac{\sigma_{L'}}{f_{L'}} - \frac{\sigma_{T'}}{f_{T'}} \right)^2 + \left(\frac{2\tau_{L'T'}}{f_{L'T'}} \right)^2 \right\}^{1/2} \quad (3)$$

where the transformed stress components are

$$\begin{aligned} \sigma_{L'} &= \sigma_L \\ \sigma_{T'} &= \sigma_T \cos^2 \theta \\ \tau_{L'T'} &= \tau_{LT} \cos \theta \end{aligned} \quad (4)$$

and the transformed stress-fringe values are

$$\begin{aligned} f_{L'} &= f_L \\ f_{T'} &= f_T \text{ (due to transverse isotropy)} \\ f_{L'T'} &= f_{LT} \text{ (due to transverse isotropy)} \end{aligned} \quad (5)$$

Therefore, Equation (3) can be rewritten as

$$N_{\theta} = \frac{h}{\cos\theta} \left\{ \left(\frac{\sigma_L}{f_L} - \frac{\sigma_T \cos^2 \theta}{f_T} \right)^2 + \left(\frac{2\tau_{LT} \cos \theta}{f_{LT}} \right)^2 \right\}^{1/2} \quad (6)$$

The stress components σ_L , σ_T and τ_{LT} can be obtained from Equations (1), (2) and (6). The principal stresses and their directions, if required, can then be obtained.

DESCRIPTION OF TESTS AND RESULTS

To verify the proposed experimental method, a 0.6 cm. thick, 30 cm. by 30 cm. composite plate was tested under a compressive edge load. The plate was fabricated from E-glass roving and a polyester resin and contained the fibers in only one direction. Two tests were conducted, one with the edge load perpendicular to the reinforcement and the other with the load parallel to the reinforcement. The elastic and photoelastic constants for the model material, incorporating 40 per cent fibers by volume, are given in Table 1.

In order to measure the isochromatic fringe order under oblique incidence, a chopped prism arrangement, shown in Fig. 2, was used. To rotate the model about the L-axis, the chopped prism was aligned with the L-direction and the fringe order N_0 on either side of the central region was measured. The angle θ was established for the model material by calibrating two tensile specimens, one with the fibers running parallel to the specimen axis and the other with the fibers perpendicular to the specimen axis. In both cases, the prism axis was aligned with the fiber direction. For the first tensile specimen $\cos\theta = N_n/N_0$ and for the second specimen $\cos\theta = N_0/M_n$. The angles were found to be 35 and 39 degrees, respectively, and an average value of 37 degrees was used for θ .

The theoretical solution for an orthotropic half-plane subjected to an edge-load is given by Lekhnitskii⁽¹³⁾. For a concentrated force P acting normal to an edge of the plate, the cartesian stress components are given by

$$\sigma_x = -\frac{P(u_1 + u_2)}{\pi hk} \cdot \frac{x^3}{(y^2 + u_1^2 x^2)(y^2 + u_2^2 x^2)} \quad (7)$$

$$\sigma_y = -\frac{P(u_1 + u_2)}{\pi hk} \cdot \frac{xy^2}{(y^2 + u_1^2 x^2)(y^2 + u_2^2 x^2)} \quad (8)$$

$$\tau_{xy} = -\frac{P(u_1 + u_2)}{\pi hk} \cdot \frac{x^2 y}{(y^2 + u_1^2 x^2)(y^2 + u_2^2 x^2)} \quad (9)$$

where the x-axis is taken along the direction of the load and the y-axis is along the loaded edge. The constant k is given by

$$k = \frac{E_L}{E_T} \quad (10)$$

when the reinforcement is perpendicular to the load and the constants u_1 and u_2 are the roots of

$$\frac{u^4}{E_T} - \frac{1}{3L_T} - \frac{2\nu_{LT}}{E_L} u^2 + \frac{7}{E_L} = 0 \quad (11)$$

Typical normal-incidence light-field isochromatic fringes corresponding to the edge load perpendicular to the fibers and parallel to the fibers are shown in Figs. 3 and 4, respectively. The cartesian stress components referred to the material symmetry axes, given by Equations (7)-(9) are shown in Figure 5 for the case when the load is perpendicular to the reinforcement. In this figure, the stress components are shown as a function of the angle from the load direction, for a radial distance of 25 mm. Also shown in the figure are the experimental values obtained from Equations (1),(2) and (6). The experimental values agree quite well with the theoretical values. Similar results, shown in Figure 6 for the case when the load is parallel to the reinforcement, also indicate good agreement between theory and experiment. In Figures 7 and 8, the stress components are shown as a function of the radial distance from the point of loading. In both cases, when the radial line makes 45° with the direction of loading, the three stress components are equal; the experimental points are not shown. Directly below the point of loading ($\theta = 0^\circ$), the stress is radial compressive and therefore the other two stress components vanish.

CONCLUSIONS

It has been shown in this paper that the state of stress at any point of a transversely isotropic birefringent model can be determined by combining the normal incidence- and the oblique incidence- isochromatic fringe orders. The procedure is greatly simplified if the model (or the light beam) is rotated about the reinforcement direction. Results from such an experimental procedure show good agreement with theoretical results for a half-plane subjected to a concentrated edge-load.

ACKNOWLEDGEMENT

This research was supported by grant no. CME-8012956 from NSF and by cooperative agreement no. NCCI-26 from NASA-LRC. The author would like to thank Dr. Clifford J. Astill of NSF and Dr. Paul A. Cooper of NASA-LRC for their support and encouragement.

REFERENCES

1. Prabhakaran, R., "Developments in Photo-Orthotropic-Elasticity," Proceedings of the I.U.T.A.M. Symposium on Optical Methods in Mechanics of Solids, Edited by A. Lagarde, published by Sijthoff and Noordhoff, 1981, pp. 559-585.
2. Prabhakaran, R., "Applications of Transmission Photoelasticity to Composite Materials," a chapter in Developments in Composite Materials, Vol. 2, Edited by G. S. Holister, to be published by Applied Science Publishers, pp. 75-99.
3. Hayashi, T., "Photoelastic Method of Experimentation for Stress Analysis in Orthotropic Structures," Proceedings of the Fourth International Symposium on Space Technology and Science, Tokyo, 1962, pp. 156-169.
4. Netrebko, V. P., "Optical Polarization Method of Studying the Stress State of Anisotropic Bodies," Mekhanika Tverdogo Tela, No. 1, 1971, pp. 94-100.
5. Netrebko, V. P., Zlenko, L. S., "Photoelastic Determination of the State of Stress and Strain in Two-Dimensional Orthotropic Bodies," Moskovski Universitet Vestnik, Seriya I-Matematika Mekhanika, Vol. 26, 1971, pp. 101-106.
6. Sampson, R. C., "A Stress-Optic Law for Photoelastic Analysis of Orthotropic Composites," Experimental Mechanics, Vol. 10, 1970, pp. 210-216.
7. Knight, C. E. and Pih, H., "Shear Difference Method and Application in Orthotropic Photoelasticity," Journal of Engineering Materials and Technology, Vol. 98, 1976, pp. 369-374.
8. Chandrasekhara, K. and Abraham, J. K., "A Numerical Method for Separation of Stresses in Photo-Orthotropic-Elasticity," Experimental Mechanics, Vol. 16, 1978, pp. 61-66.
9. Chandrasekhara, K. and Abraham, J. K., "An Experimental-Numerical Hybrid Technique for Stress Analysis of Orthotropic Composites," Developments in Composite Materials, Vol. 1, Edited by G. S. Holister, published by Applied Science Publishers.
10. Rowlands, R. E., Dudderar, T. D., Prabhakaran, R. and Daniel, I. M., "Holographically Determined Isopachics and Isochromatics in the Neighborhood of a Crack in a Glass-Composite," Experimental Mechanics, Vol. 20, 1980, pp. 53-56.
11. Prabhakaran, R., "Separation of Principal Stresses in Photo-Orthotropic Elasticity," Fibre Science and Technology, Vol. 13, 1980, pp. 245-253.
12. Prabhakaran, R., "Determination of Principal Stresses in Birefringent Composites by Hole-Drilling Method," Proceedings of the 36th Annual Conference, Society of the Plastics Industry, 1981, Session 10-C.
13. Lekhnitskii, "Anisotropic Plates," Translated by S. W. Tsai and T. Cheron from Russian into English, Gordon and Breach Science Publishers, New York, 1968.

LIST OF FIGURES

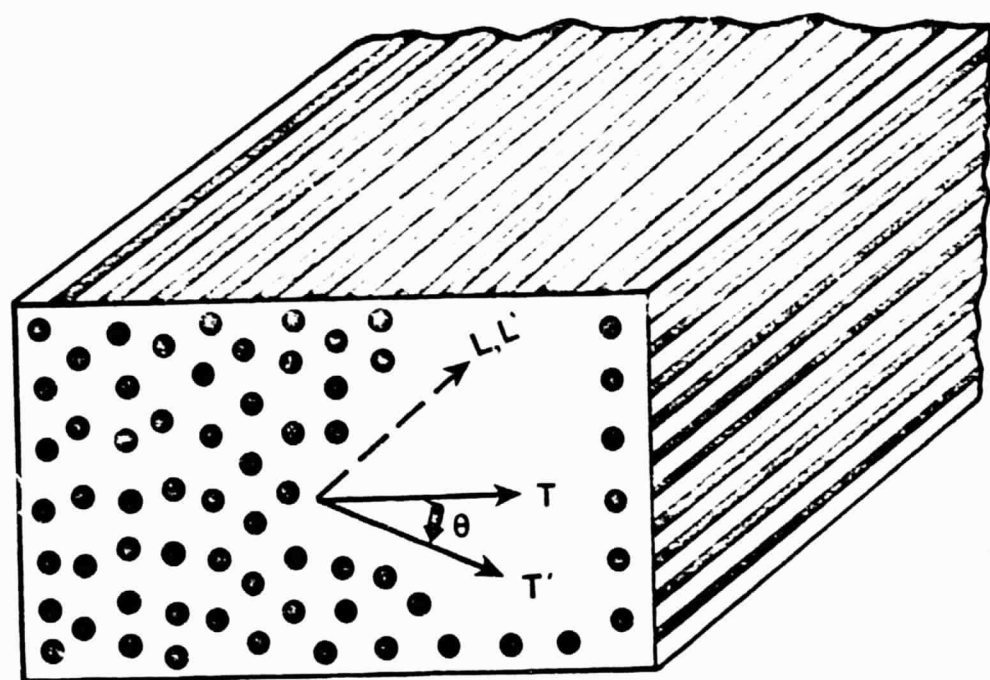
- Figure 1. Coordinate axes and their transformation under oblique incidence.
- Figure 2. Chopped prism oblique incidence arrangement.
- Figure 3. Normal-incidence light-field isochromatic fringe pattern for loading perpendicular to the reinforcement.
- Figure 4. Normal-incidence light-field isochromatic fringe pattern for loading parallel to the reinforcement.
- Figure 5. Stress components as a function of angle from the load-direction for loading transverse to the reinforcement.
- Figure 6. Stress components as a function of angle from the load-direction for loading parallel to the reinforcement.
- Figure 7. Stress components as a function of the radial distance from the point of loading for loading transverse to the reinforcement.
- Figure 8. Stress components as a function of radial distance from the point of loading for loading parallel to the reinforcement.

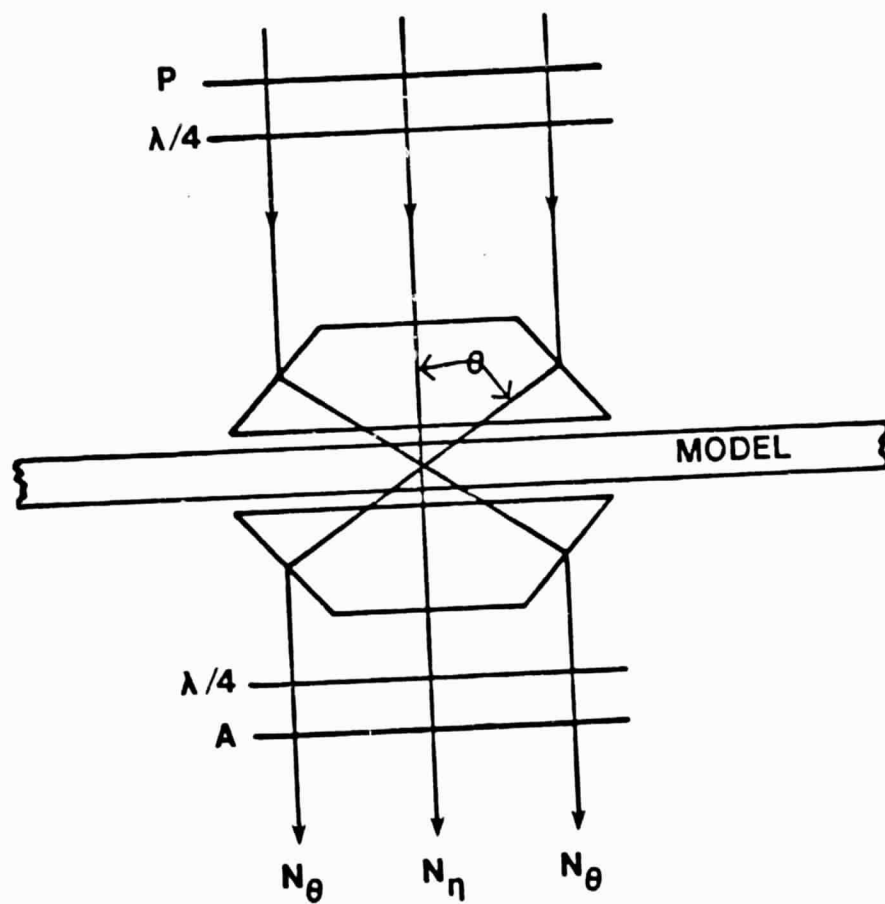
LIST OF TABLES

Table 1. Elastic and photoelastic properties of birefringent composite model

TABLE 1 ELASTIC AND PHOTOELASTIC PROPERTIES OF BIREFRINGENT COMPOSITE MODEL

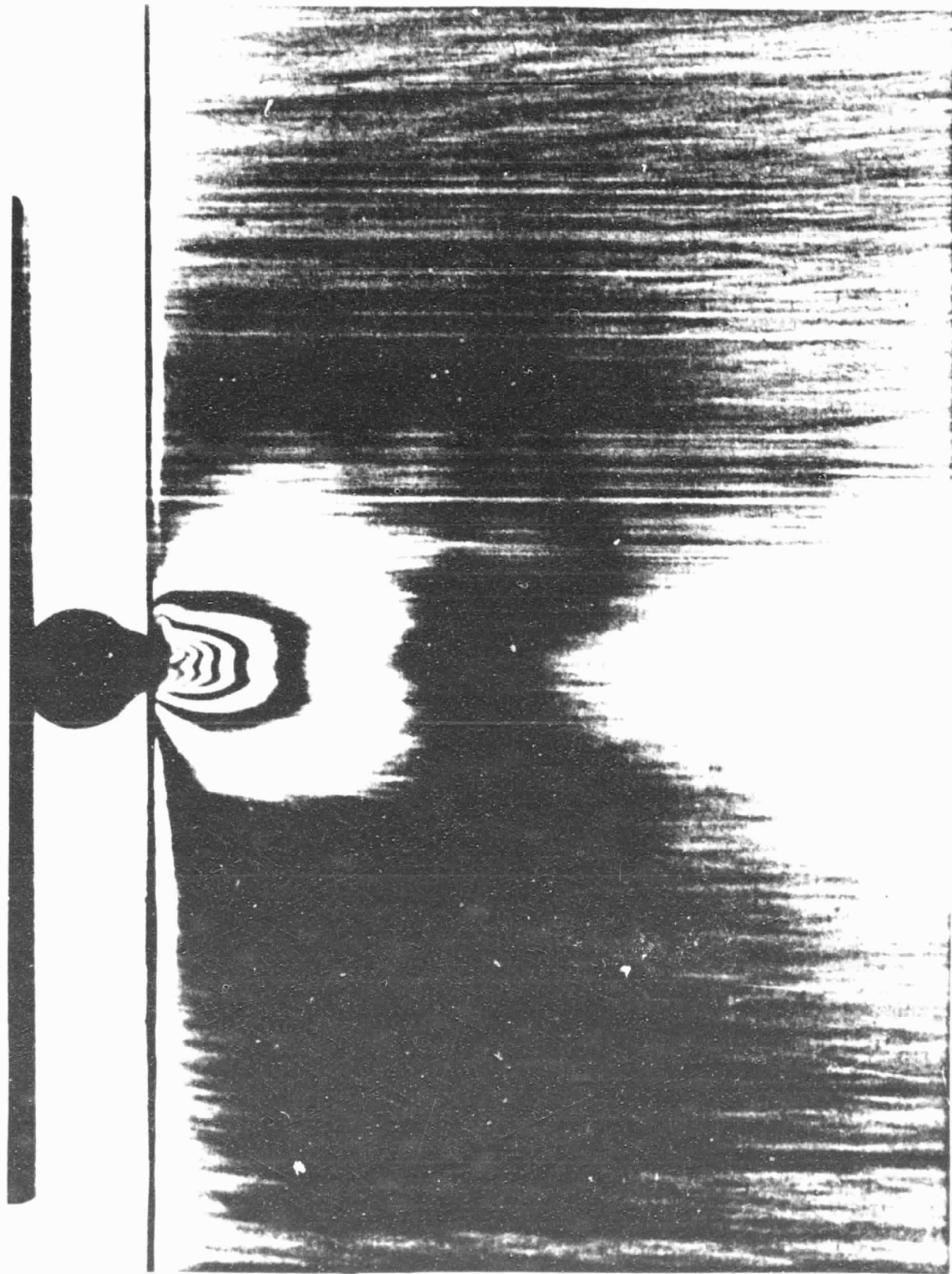
<u>Property</u>	<u>Value</u>
E_L	28.8 GPa
E_T	9.4 GPa
G_{LT}	3.2 GPa
ν_{LT}	0.3
f_L	156 KPa-m/fringe
f_T	78 KPa-m/fringe
f_{LT}	69 KPa-m/fringe

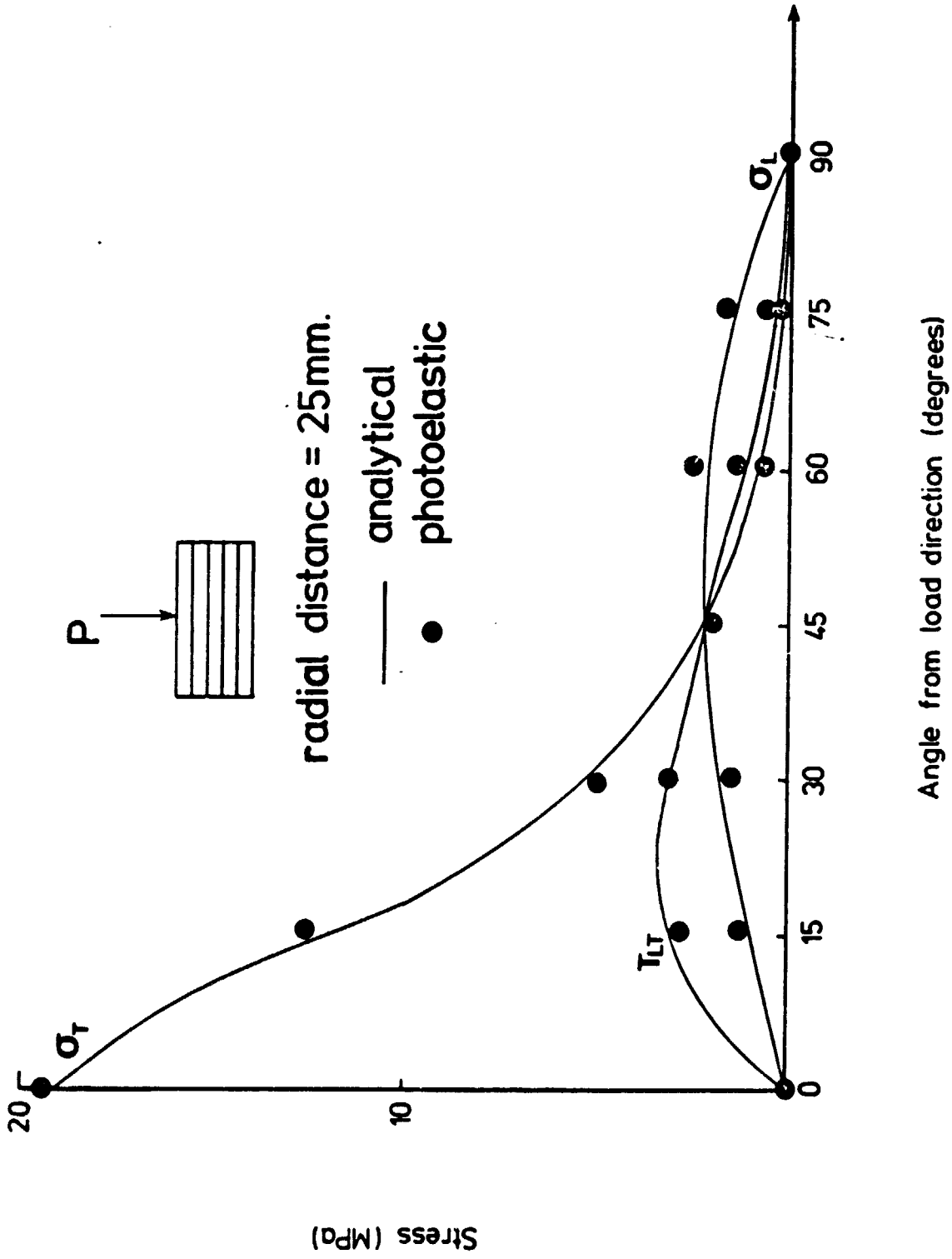


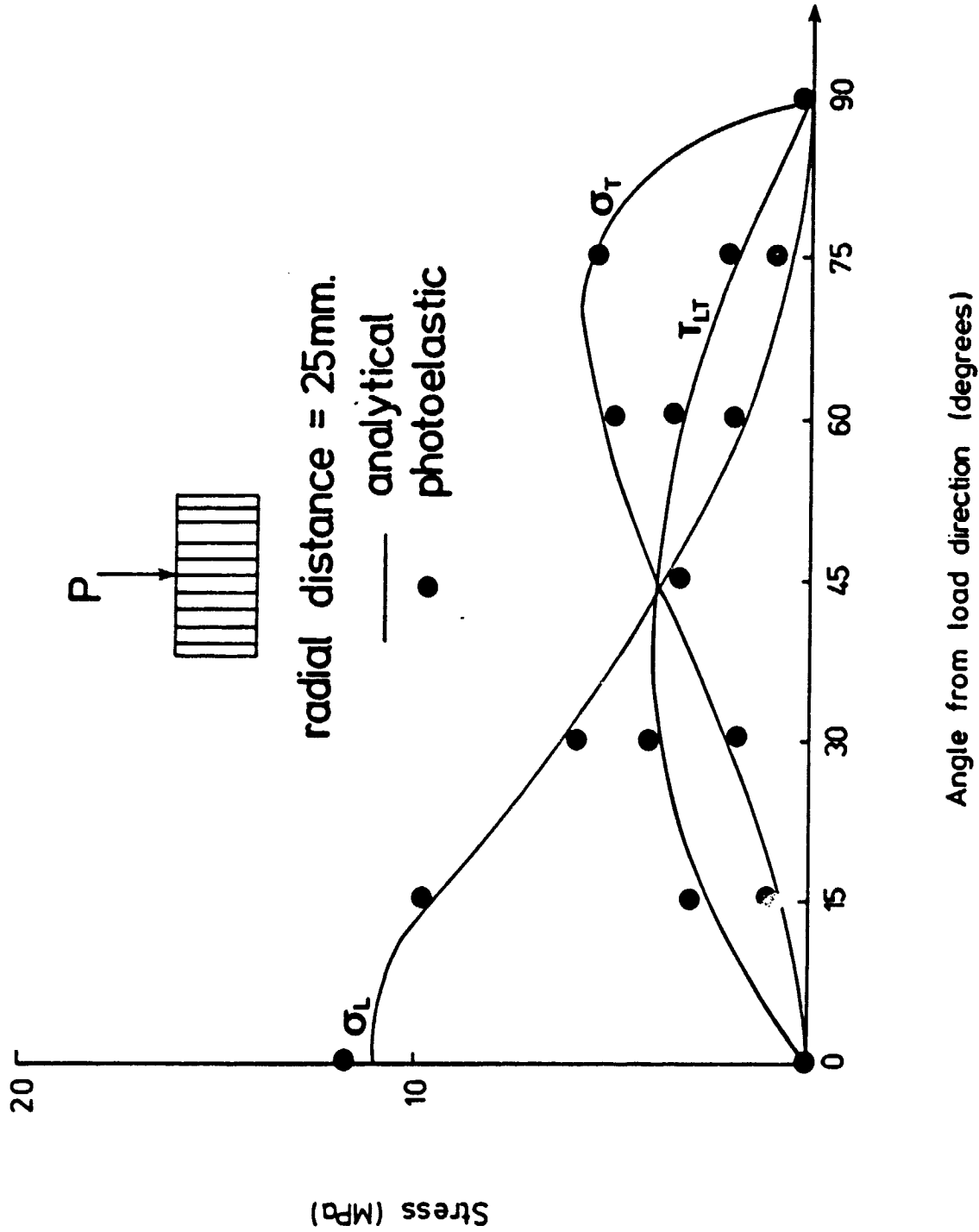


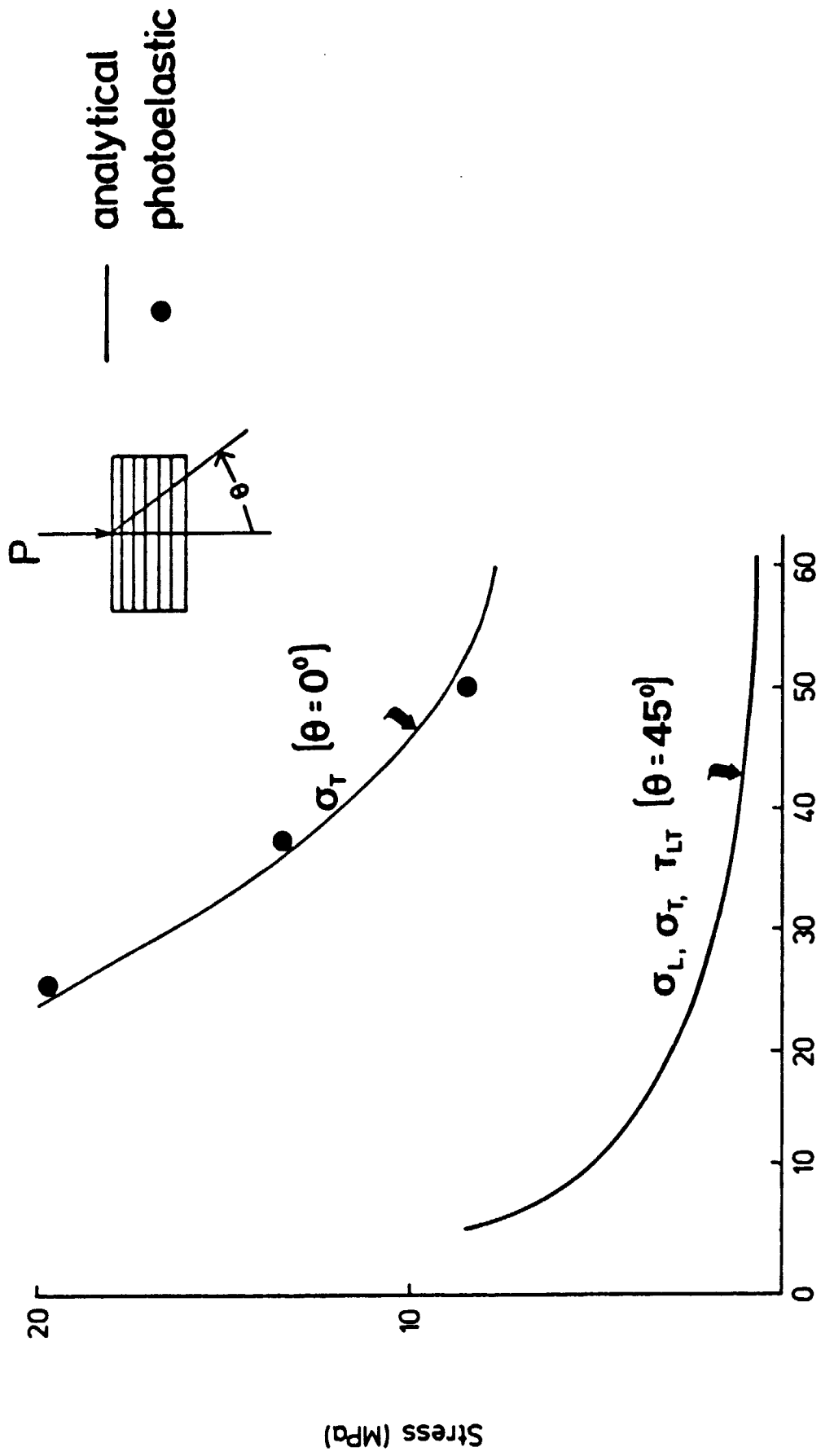


ORIGINAL PAGE IS
OF POOR QUALITY

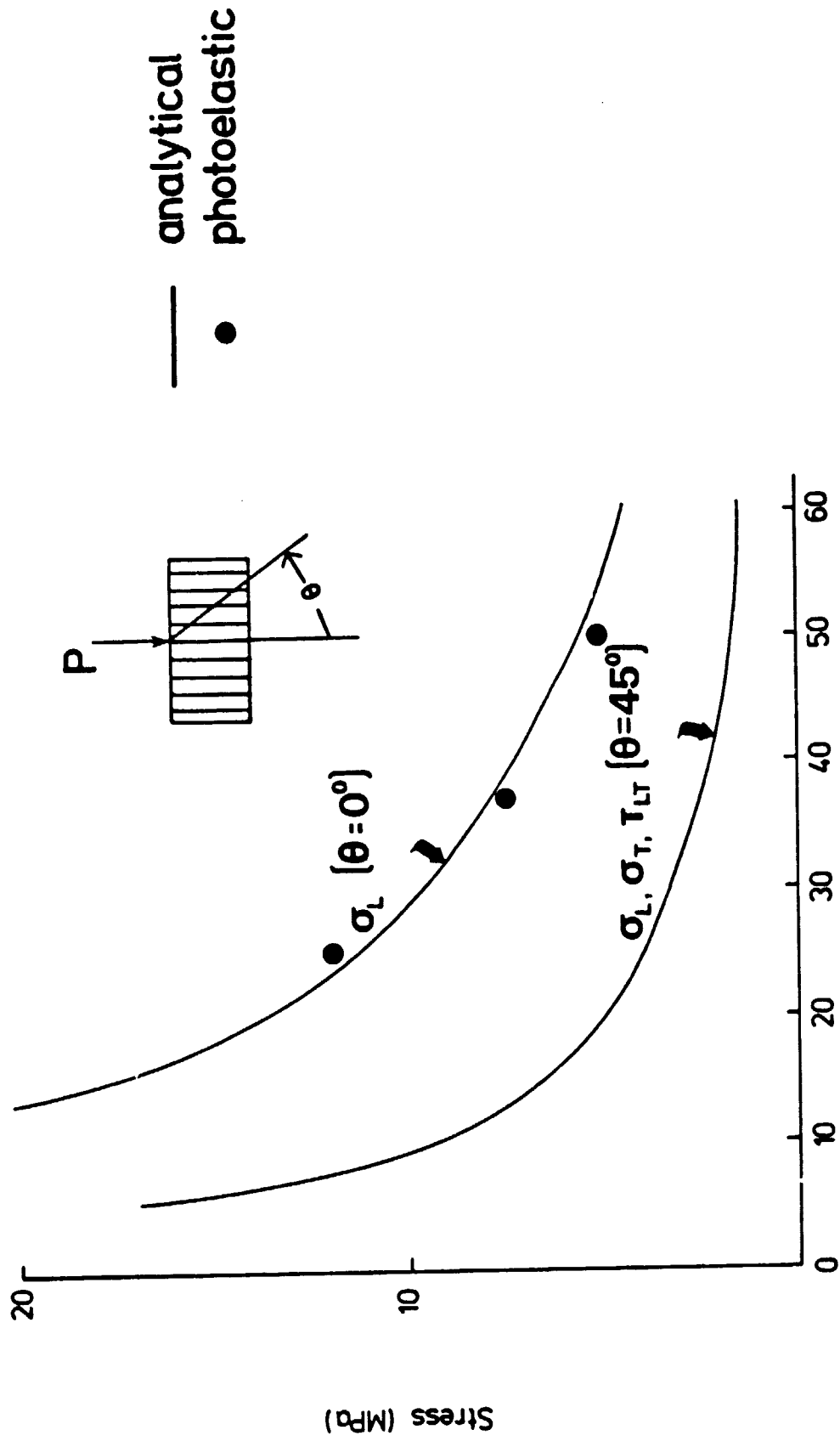








Radial distance from point of loading (mm)



Radial distance from point of loading (mm.)